Energy Transmission by Barotropic Rossby Waves Revisited

R. P. MATANO

College of Oceanic and Atmospheric Sciences, Oregon State University, Corvallis, Oregon

E. D. PALMA

Departamento de Física, Universidad Nacional del Sur, Bahia Blanca, Argentina

(Manuscript received 4 May 2004, in final form 11 May 2005)

ABSTRACT

This article presents a semianalytic method to investigate the properties of energy transmission across bottom topography by barotropic Rossby waves. The method is first used to revisit the analytical estimates derived from wave-matching techniques and Wentzel–Kramers–Brillouin (WKB) approximations. The comparison between the semianalytic method and WKB indicates that the results of the latter are valid for waves with periods longer than a month and ridges taller than ~1000 m and wider than ~500 km. For these parameter values both methods predict the passage of low-frequency waves and the reflection of high-frequency waves. The semianalytic method is then used to discuss the energy transmission properties of a cross section of the Mid-Atlantic Ridge. It is shown that the filtering characteristics of realistic bottom topographies depend not only on the spatial scale set by the cross-section envelope, but also on the scales of the individual peaks. This dependence is related to the fact that topographies narrower than ~400 km (e.g., peaks) are high-pass filters of incoming waves, while topographies wider than that (e.g., cross-section envelopes) are low-pass filters. In the particular case of the Mid-Atlantic Ridge the neglect of the contribution of individual peaks leads to an erroneous estimate of the filtering properties of the massif.

1. Introduction

The adjustment of the large-scale, oceanic circulation to the atmospheric forcing at intra-annual time scales is largely accomplished by the generation and propagation of barotropic Rossby waves. The propagation of these waves, however, is strongly influenced by the topography of the ocean floor. Ridges and seamounts attenuate barotropic modes of a wide range of frequencies while a rough bottom may prevent any wave propagation. The influence of the bottom topography on the transmission of energy by barotropic Rossby waves was first investigated by Rhines (1969) and Barnier (1984). In these studies the bottom of the ocean was represented by simple exponential or step functions, and the solutions to the potential vorticity equation were derived by matching plane waves at the boundaries of regions of constant ambient vorticity gradients. Most of what we know about these matters has been derived from these simple and insightful models. In a relatively more recent study Matano (1995, M95 hereinafter), derived an analytical solution for the potential vorticity equation using the Wentzel–Kramers–Brillouin (WKB) method and compared it with the results of numerical simulations.

Although the solutions derived from the analytic (wave matching and WKB) and the numerical models are qualitatively meaningful, their implications for realistic bottom configurations are obscured by the formal limitations of the solution method. The analytical models can only be applied to highly unrealistic types of bottom topography. The numerical results can bypass this constraint but their results are influenced by unwanted (but difficult to remove) factors such as the shape of basin (which lead to the excitation of a particular set of basin modes), the propagation of gravity and boundary waves, the details of the wave-forcing mechanism, and so on. To circumvent these limitations in this article we present a semianalytical model that solves the potential vorticity equation discussed in M95, with the addition of a set of matching conditions that

Corresponding author address: Dr. Ricardo P. Matano, College of Oceanic and Atmospheric Sciences, Oregon State University, Corvallis, OR 97331-5503.
E-mail: rmatano@coas.oregonstate.edu

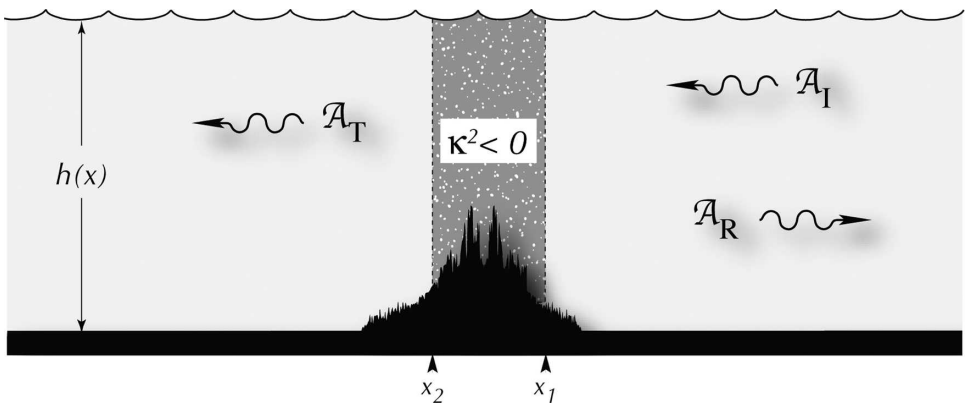

FIG. 1. Schematic representation of Rossby wave propagation in an ocean basin of constant depth divided by a meridional ridge. Wave propagation is inhibited in the region limited by x_1 and x_2.

render the problem amenable to the use of numerical methods. The objective of this exercise is twofold; first, we want to determine the range of validity of the analytical and numerical solutions, and second, we want to determine the energy transmission properties of slightly more realistic topographic profiles than in previous studies.

2. The model

Let's consider the linear, quasigeostrophic dynamics of a homogenous, inviscid, ocean basin consisting of two regions of constant depth separated by a meridional ridge of unspecified shape (Fig. 1). In the eastern side of the basin there is a westward-propagating wave packet (of unit amplitude) that, after impinging on the ridge, generates reflected and transmitted wave packets. This dynamical system is described by the potential vorticity equation for the mass streamfunction, which, after some canonical transformations, leads to the following set of equations (e.g., LeBlond and Mysak 1978; M95):

$$\phi(x) = \begin{cases} e^{ik_I x} + A_R e^{ik_R x} & x > x_2 \\ \dfrac{d^2\phi}{dx^2} + \kappa^2(x)\phi = 0 & x_1 < x < x_2, \\ A_T e^{ik_I x} & x < x_1 \end{cases} \quad (1)$$

where $\phi(x)$ is the zonal component of the mass streamfunction $\psi(x, y, t)$; that is,

$$\psi(x, y, t) = \phi(x) h^{1/2} \exp\left[i\left(-\frac{\beta}{2\omega} x + ly - \omega t \right) \right] \quad (2)$$

and

$$\kappa^2(x) = \left(\frac{\beta}{2\omega} \right)^2 - l^2 - \frac{fl}{\omega} \frac{h_x}{h},$$

where β is the gradient of planetary vorticity, ω is the frequency of the propagating wave, l is the meridional wavenumber, k_I and k_R are the zonal wavenumbers of the incident and reflected waves, and $h(x)$ is the bottom depth. Given ω and l, k_I and k_R can be calculated from the dispersion relation. The solutions to the above system depend on the value of the potential $k^2(x)$. If $k^2(x)$ is positive (and a slowly varying function) then the only effect of the bottom topography on the wave propagation is a local refraction of the wave packet with no associated energy reflection. If, however, $k^2(x)$ is negative somewhere in the domain, then the solutions to (1) decay exponentially in that region and the topography represents a barrier to the energy transmission. The amount of energy that can be transmitted across this portion of the domain depends on the shape of the bottom and the frequency and direction of the incident waves.

System (1) has been solved analytically using wave-matching techniques for topographic profiles of constant slope (e.g., Rhines 1969; Barnier 1984), and the WKB technique for more general forms of bottom topography (M95). The validity of these solutions, however, is strongly limited by the approximations made by the solution method. The wave-matching technique, for example, requires the use of topographic profiles with unrealistic slopes. The WKB solution is more general but it requires that the wavelength of the incident wave be smaller than the scale of the bottom topography. Since even relatively short, nondivergent, barotropic waves have wavelengths comparable to, or greater than, the scale of the bottom topography, the formal validity of a WKB solution is marginal at best. M95 made a qualitative comparison between the values predicted by (2) and the results of a primitive equation model. The comparison, however, was obscured by the

fact that the numerical model encompassed a wider gamut of processes than those represented by (1). Given these considerations and in order to gain further understanding on the energy transmission properties of barotropic Rossby waves, herein we will solve (1) directly using a numerical method. To do so we need to impose the following boundary conditions at the limits of the region where $k^2(x)$ is negative; that is, at $x = x_1$:

$$\phi(x_1) = A_T e^{ik_T x_1} \quad \text{and}$$

$$\frac{d\phi}{dx}(x_1) = ik_I \phi(x_1),$$

and at $x = x_2$:

$$\phi(x_2) = e^{ik_I x_2} + A_R e^{ik_R x_2} \quad \text{and}$$

$$\frac{d\phi}{dx}(x_2) = ik_I e^{ik_I x_2} + ik_R e^{ik_R x_2} A_R e^{ik_R x_2}$$

$$= i(k_I - k_R) e^{ik_I x_2} + ik_R \phi(x_2). \tag{3}$$

Equations (1) and (3) form a closed system that was separated into its real and imaginary components and solved numerically using the *shooting* technique (Press et al. 1992). We make an initial guess of the values of the imaginary component of ϕ to compute the real component from the boundary conditions at x_1. We then integrate (1) from the boundary conditions at x_1 to those at x_2 and construct a discrepancy vector that measures the degree of satisfaction of the boundary conditions at $x = x_2$. This is used to adjust the values of the imaginary components at x_1 to attain the desired level of tolerance in satisfying the boundary conditions at x_2 and accuracy using the globally convergent Newton method (Press et al. 1992). Once the specified accuracy has been achieved, the solution is complete and accurate to the level of tolerance chosen and to the order of the time-stepping scheme.

3. Solutions

a. Bottom topographies of constant slope

Rhines (1969) investigated the case of two flat-bottomed basins connected by a step of exponential shape and width a. The coefficient of energy transmission derived for that particular case is

$$T = \left[1 + 0.25\left(\frac{\mu}{\kappa} + \frac{\kappa}{\mu}\right)^2 \sinh^2(\mu a)\right], \tag{4}$$

where $\delta = h_1/h_2$, and $\mu^2 = -\kappa^2 - l\delta/\omega a$.

To compare (4) with the numerical solution described in the previous section we calculated the transmission coefficients as a function of the frequency and the step width for a basin with a fractional depth change $\delta = 0.05$ (Fig. 2). The transmission coefficients for basins with other fractional depth changes are qualitatively similar. The amount of transmitted energy decreases as the fractional depth change increases (Fig. 2). As noted by Rhines the energy transmission is largely insensitive to the step width until $(\omega/\delta)ka \sim 1$, and it decreases with decreasing frequencies. The difference between the analytical and numerical solution is negligible for all the values of δ that we tested.

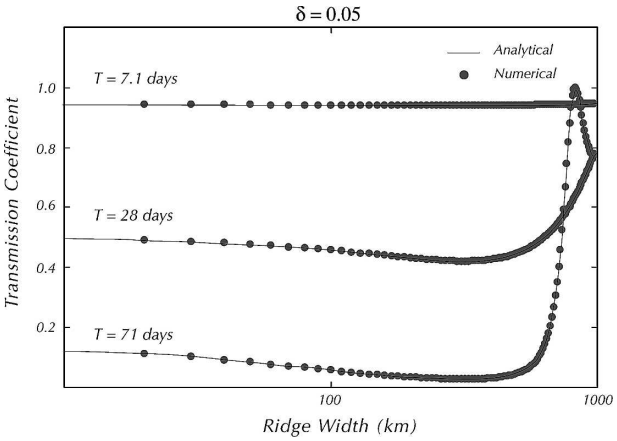

FIG. 2. Transmission coefficient for a step topography as a function of the step width. The incident wave has $k = l$.

To further probe the numerical method we determined the energy transmission properties of a flat-bottomed basin divided by a meridional ridge shaped by the intersection of two exponentials. Barnier (1984) derived an analytical expression for this particular case, and we compared his expression with the results derived from the numerical calculation (Fig. 3). As in the previous case, there is good agreement between analytical and numerical results. Both methods indicate that the energy transmission is more efficient at low frequency and that the frequency at which waves can cross the topography without any energy reflection shifts toward smaller values as the parameter $\delta f/\beta a$ increases (not shown).

b. A Gaussian ridge

The analytical examples discussed in the previous section were restricted to bottom topographies of constant slope. M95 derived the following solution for topographies with variable slopes:

$$T = \frac{1}{|A_T|^2} \cong \exp\left\{\int_{x_1}^{x_2} \sqrt{\left[\left(\frac{\beta}{\omega}\right)^2 - l^2 - \frac{fl}{\omega}\frac{h_x}{h}\right]}\, ds\right\}. \tag{5}$$

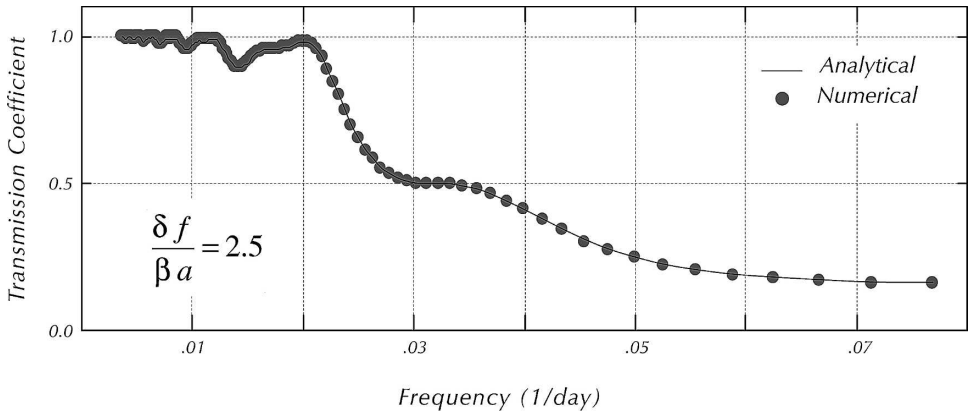

FIG. 3. Transmission coefficient as a function of the frequency for a meridional ridge shaped by exponential functions.

Although this expression is more general than the expressions derived by Rhines and Barnier, it requires that κ^2 be a slowly varying function of the zonal coordinate, a requirement that is not always fulfilled in the real ocean. To determine the range of validity of WKB in this section we compare (5) with the results of the semianalytical model. To that end we consider the energy transmission properties in a 4000-m-deep basin divided by Gaussian ridges of varying shapes (Fig. 4a). There is good agreement between WKB and the semianalytical method for waves with periods longer than a month ($\omega \sim 0.03$), and for ridges taller than ~1000 m. WKB, however, underestimates the *tunneling* process that allows relatively shorter waves to pass through the potential barrier. There is, for example, a large discrepancy between the energy transmission predicted by WKB and the semianalytical method for a 500-m-tall ridge. The agreement, however, improves substantially if the cross section of the ridge is augmented from 500 to 1500 km (Fig. 4b). The above results therefore, suggest that (5) is valid for waves with periods longer than a month and ridges taller than ~1000 m and wider than ~500 km.

The transmission coefficients derived from the semianalytical model are less restricted than those using the WKB approximation. They are, nevertheless, constrained by the idealizations involved in their derivation. It is desirable, therefore, to compare the semianalytical results with those of a more general model. For these purposes we use the energy transmission coefficients calculated by M95 using a nonlinear, shallow-water model on a rotating sphere. The model domain consisted of a rectangular basin, 200° long, 60° wide, and centered at 40°N. The bottom depth was constant everywhere (4000 m), except the middle where there was a meridional ridge of Gaussian shape. To generate westward-propagating waves the model was forced with an idealized wind stress specification near the eastern boundary. The energy transmissions in different regions of the model were calculated as the ratio between the kinetic energy associated with a specific ridge configuration and the kinetic energy corresponding to a flat-bottomed basin.

Before discussing the results it should be noted that, since the semianalytical and the numerical models encompass different dynamical ranges, it is not straightforward to compare them. The semianalytical model, on the one hand, focuses on the linear dynamics of Rossby waves in an infinite (unbounded) domain. The M95 model, on the other hand, not only included Rossby waves but also gravity and boundary waves, basin modes, nonlinear interactions (but at such small Rossby number that these terms do not measurably influence wave propagation characteristics), bottom friction, and so on. The coefficient of friction near the western boundary was smoothly increased to 100 times its value in the open ocean to avoid unwanted reflections of short, eastward-propagating Rossby waves. Despite these differences our calculation shows a reasonable agreement between the energy transmission coefficients derived from both methods (Fig. 5). The estimates from the numerical model lack some of the qualitative details of the semianalytical and WKB solutions, such as the frequency dependence of the energy transmission coefficient (a fact that can be partly attributed to the limited frequency range that was resolved in that simulation), but are quantitatively similar. Both methods, for example, predict that a 1000-m ridge will allow the passage of approximately 35% of the incoming energy for waves with periods less than 3 months, while a 1500-m ridge will allow the passage of only 15%. The general agreement between these estimates and their

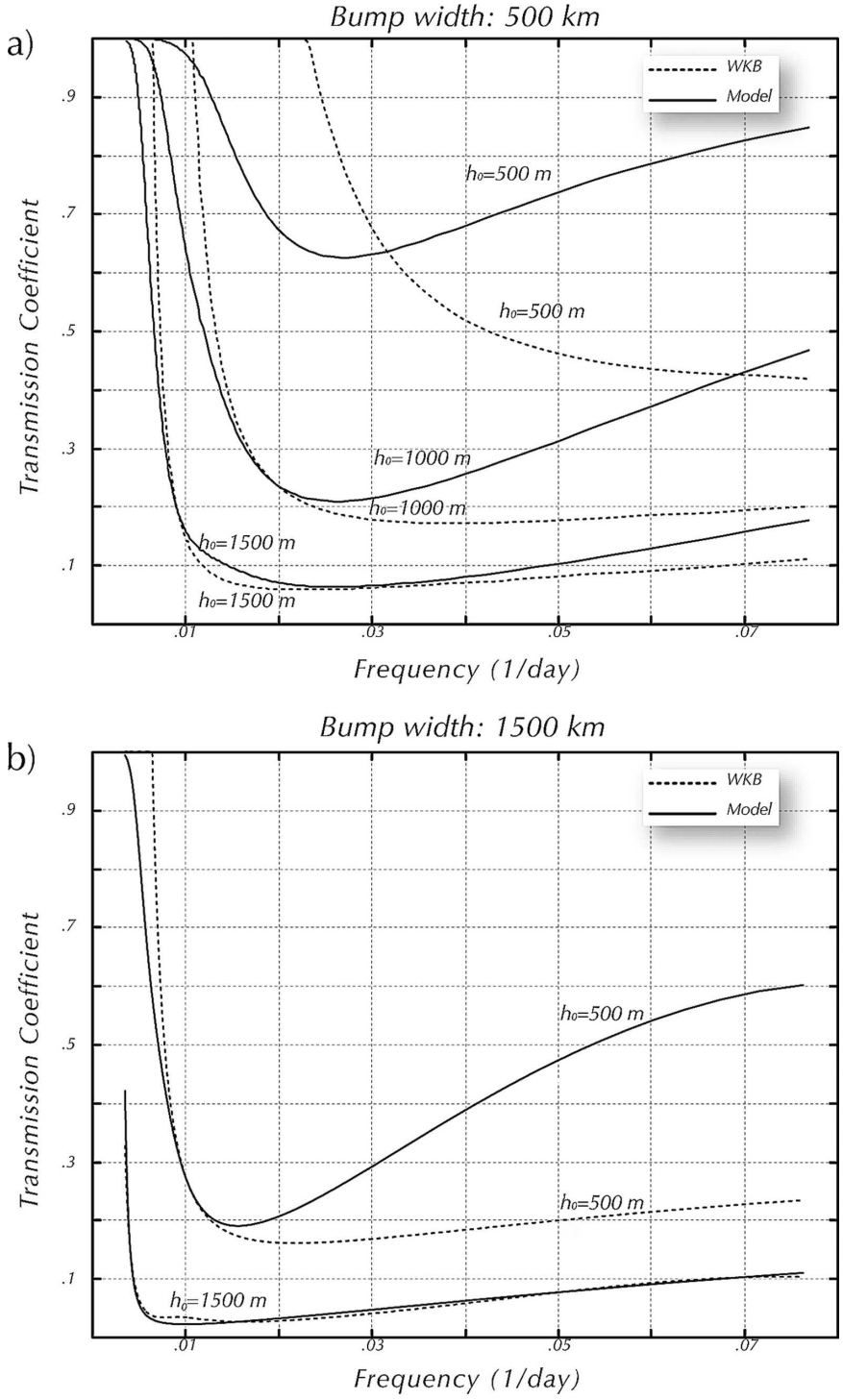

FIG. 4. Transmission coefficients calculated from the numerical method (solid line) and from the WKB approximation (dotted line). These curves correspond to a Gaussian bump of height h_0 and cross-sectional width of (a) 500 and (b) 1500 km.

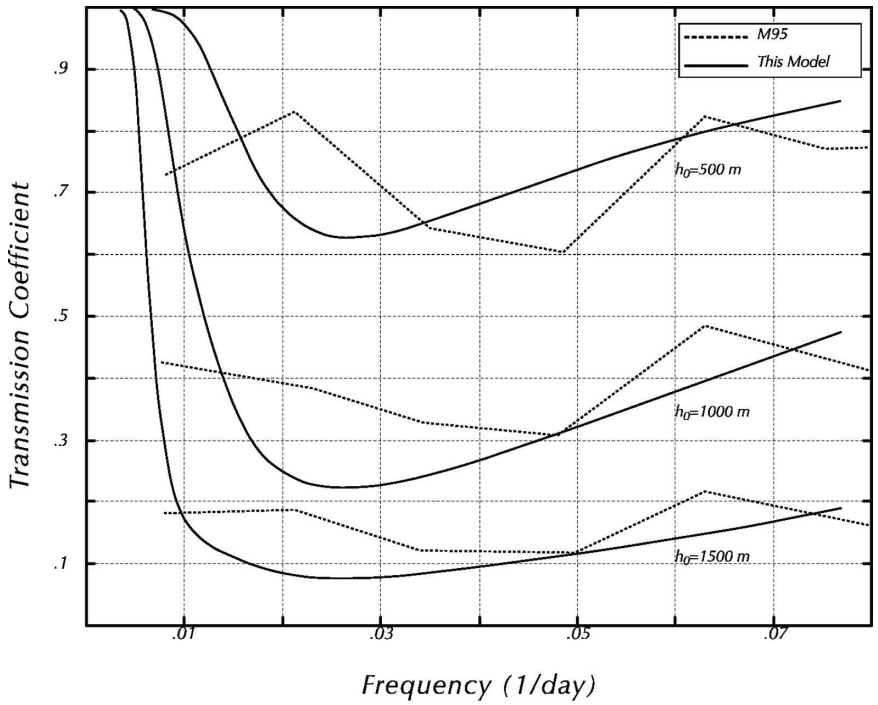

FIG. 5. Transmission coefficients calculated from the semianalytical model (solid line) and from the numerical simulation of M95. The bottom topography was represented by a Gaussian bump of height h_0 and cross-sectional width of 500 km.

closeness to the values predicted from WKB (Fig. 4) indicates that the above results are relatively robust.

Since the semianalytical solutions are more general than those obtained through WKB and have fewer encumbrances than those generated by the numerical model, we used them to investigate the sensitivity of the energy transmission coefficient to the meridional wavelength, the ridge width, and latitude (Figs. 6,7,8). The influence of the meridional wavenumber on the energy transmission properties is greater at the low-frequency end of the spectrum (Fig. 6). For a fixed frequency the transmission coefficient increases with the meridional

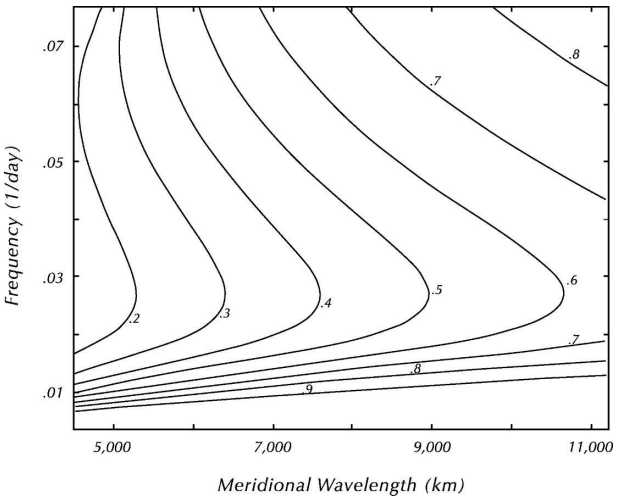

FIG. 6. Transmission coefficient for a Gaussian bump with a cross-sectional width of 500 km and a height of 500 m.

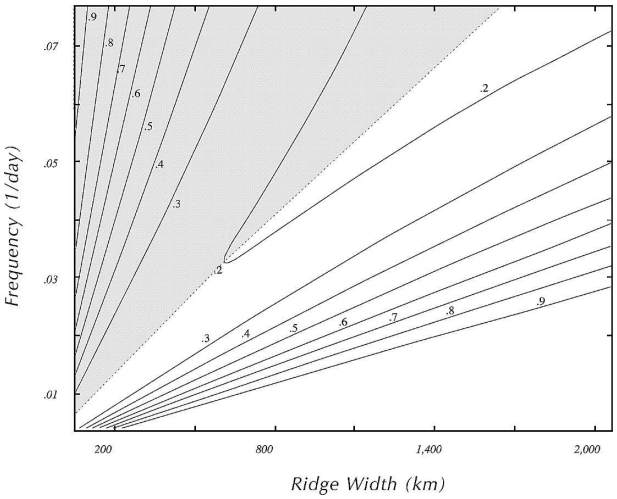

FIG. 7. Transmission coefficient as a function of the cross section for a Gaussian bump with a height of 1000 m. The stippled region marks the parameter values for which the energy transmission increases with increasing frequency. Note that cross sections narrower than ~200 km are high-pass filters.

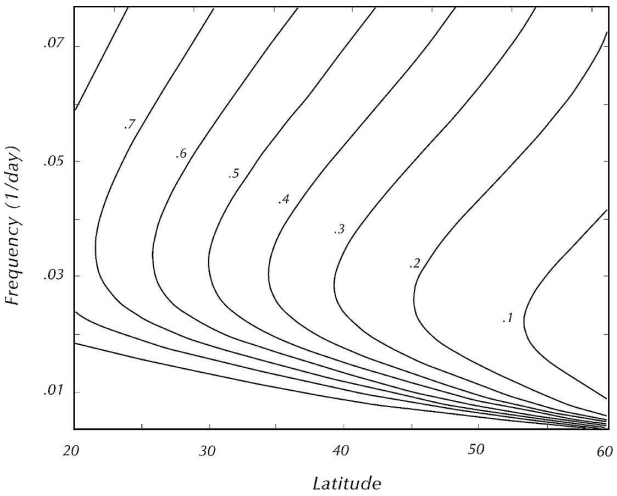

FIG. 8. Transmission coefficient as a function of the latitude for a Gaussian bump with a height of 1000 m and a cross-sectional width of 500 km.

wavelength. In the limit of $l = 0$ the particles motion is parallel to the isobaths and the wave does not feel the bottom topography. The qualitative effect of the cross-sectional width on the magnitude of the energy transmission coefficient was discussed in the previous paragraphs but its quantitative influence is illustrated here (Fig. 7). For a given frequency, a wider ridge does not necessarily lead to larger transmission coefficient but, in fact, a relatively small widening of a narrow ridge leads to a decrease of the energy transmission coefficient. In this regard it should be noted that, since the influence of the ridge cross section on the energy transmission properties is given by the term of $h^{-1}\partial h/\partial x$ in (5), the range of cross-sectional widths in which the energy transmission decreases/increases depends on the particulars of the topographic profile. The parameter range displayed in the above example only applies to a ridge of Gaussian shape. It is important to note, however, that for relatively narrow ridges (cross sections smaller than ~500 km), the energy transmission only increase with increasing frequencies (the limit discussed by Rhines 1969). For a given height, therefore, there is a threshold cross section beyond which low-frequency waves are more efficient in transporting energy than high-frequency waves. The value of that threshold not only depends on the shape of the ridge but also on its location (Fig. 8).

c. The Mid-Atlantic Ridge

The common trait of most of the figures discussed in the previous section is that the energy transmission appears to be more efficient at lower frequencies. This characteristic reflects the dominance of the ω^{-2} term [see (5)] in ridges with a relatively wide cross section ($\gtrsim$500 km). The sensitivity study, however, also indicates that a narrow ridge can prevent the propagation of low-frequency waves (Fig. 7). The question, therefore, is what are the transmission properties of realistic topographic profiles where narrow and wide peaks are found side by side? Although there is no general answer to that question because the transmission properties depend on the specifics of the topography, in this section we consider the particular case of a Mid-Atlantic Ridge cross section. This example not only allows us to investigate the properties of more realistic topographic profiles than those analyzed hitherto but also illustrates the shortcomings of highly idealized topographies. To facilitate the comparison between the analytical and semianalytical methods we fitted a Gaussian profile to the Mid-Atlantic Ridge and calculated its energy transmission properties using both methods (Fig. 9).

There is reasonable good agreement between the energy transmission coefficients estimated from WKB and the semianalytical model for the Gaussian topography (Fig. 10). Both methods predict the passage of little energy for waves with frequencies higher than ~0.015 days^{-1}, and uniformly large values for waves with frequencies lower than that. Interestingly, however, the predictions from the Gaussian topography are completely out of phase with those using the realistic cross section. In fact, for that case, the semianalytical model predicts that high-frequency waves ($\omega \gtrsim 0.05$ days^{-1}) will be able to transmit between 60% and 80% of the incoming energy, while most of the energy at the low-frequency range will be reflected back. The dis-

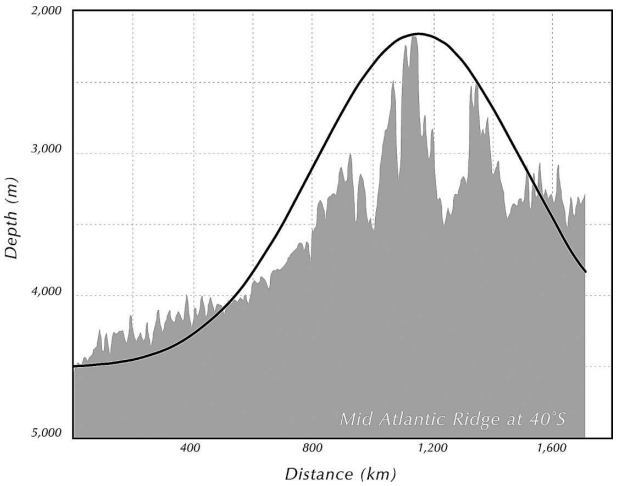

FIG. 9. Cross-sectional width of the Mid-Atlantic Ridge at 40°S and its approximate representation using a Gaussian function.

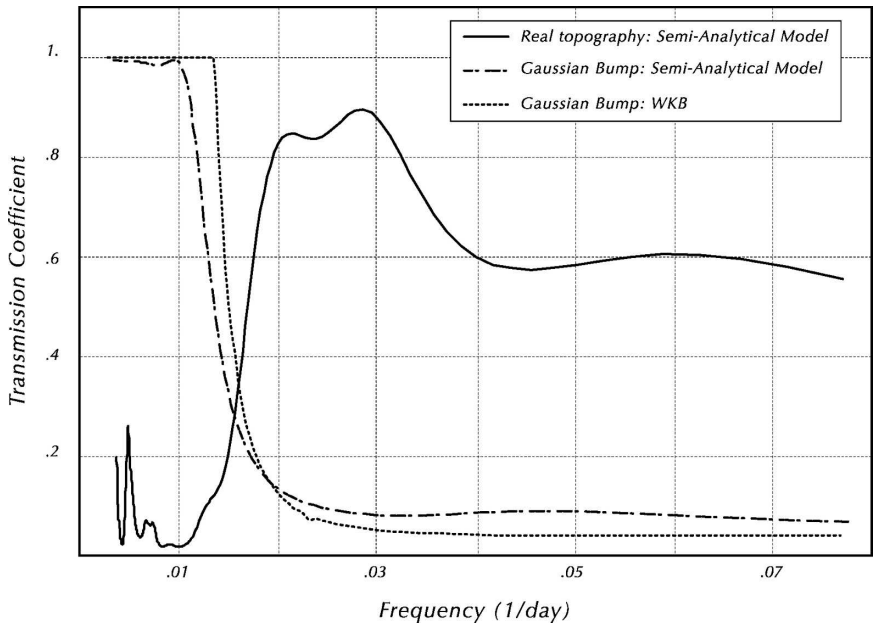

FIG. 10. Transmission coefficients for the topographic profiles depicted in Fig. 9.

crepancy between the energy transmission coefficients for the idealized and the realistic topography can be understood in terms of the ridge width. According to our previous discussion, the filtering properties of a narrow ridge are qualitatively different from those of a wide ridge; a narrow ridge is a high-pass filter of the incoming energy, while a wide ridge is a low-pass filter (Fig. 7). In these regards it should be noted that, while the idealized topographies have cross sections of approximately 800 km ("wide" ridge), the individual peaks of the realistic case have cross sections smaller than ~200 km ("narrow" ridge). The Mid-Atlantic Ridge can be thought of as the superposition of several narrow ridges and, to the extent that the individual peaks do not blend into a large massif but conserve their characteristics (i.e., to the extent that they are able to impose a specific spatial scale to the problem), they determine the properties of the energy transmission. As this example illustrates, this can lead to a radically different answer than that expected from an idealized representation of the same topographic cross section.

4. Summary and discussion

In this article we presented a semianalytic method to investigate the properties of energy transmission across bottom topography by barotropic Rossby waves. The method was first used to revisit previous analytical estimates of energy transmission using wave-matching methods (Rhines 1969; Barnier 1984) and then to evaluate the range of validity of the WKB solutions derived in M95. This exercise shows that the WKB estimates are applicable to waves with periods longer than a month and ridges taller than ~1000 m and wider than ~500 km. For these topographies WKB and the semianalytical method predict the passage of low-frequency waves and the reflection of high-frequency waves. In the last portion of this article we used a cross section of the Mid-Atlantic Ridge to investigate the properties of energy transmission across more realistic topographic shapes. There, it was shown that the filtering characteristics of the bottom topography are highly dependent on the dominant scales of the topography. This dependence is related to the fact that topographies narrower than ~400 km (e.g., peaks) are high-pass filters of incoming waves, while topographies wider than that (e.g., cross-sectional envelopes) are low-pass filters. In the particular case of the Mid-Atlantic Ridge the neglect of the contribution of individual peaks leads to an erroneous estimate of the filtering properties of the massif.

Although the Mid-Atlantic Ridge example discussed in the previous section includes scales smaller than those strictly allowed by the assumptions of the method, it serves to illustrate the dependence of the solution on the scale of the problem. It is, of course, possible to improve the fit between the Gaussian profile and the realistic cross section by increasing the smoothing in the cross section, or by including several "bumps" in the idealized shape. In those cases, how-

ever, the realistic cross section becomes less realistic and the idealized bump less idealized. The purpose of the exercise, however, was not to estimate the exact values of the energy transmission coefficients at any specific location, but rather to illustrate the importance of the cross-sectional scale in a slightly less abstract setting than that discussed in section 3b.

The semianalytical model discussed herein intends to fill the gap between theory and numerical results. A one-dimensional model, nevertheless, is a gross simplification of the real ocean. To interpret observations we need to consider the 3D nature of the wave field as well as the interactions between barotropic and baroclinic modes. The complexity of the problem, unfortunately, grows rapidly with the realism of our model so that analytical solutions are difficult to obtain and numerical results are difficult to interpret. During the last few years, however, there have been significant advances in our understanding of the influence of ridges that vary in the meridional as well in the zonal direction. Pedlosky and Spall (1999) and Pratt and Spall (2003), for example, found barotropic solutions to topographic barriers with open gaps (a configuration that might, for example, represent an island chain). Their results indicate that the islands between the gaps act as antennae that radiate the incoming energy so that a meridional barrier becomes nearly transparent to the passage of Rossby waves. Pedlosky (2000) investigated the baroclinic equivalent of this problem and considered a gap that extends to middepth (instead of reaching the full water column) and concluded that the interaction of modes at the ridge leads to a conversion energy from the baroclinic to the barotropic mode. Thus, topographic interactions tend to favor the dominance of barotropic variability on the western side of meridional ridges.

Acknowledgments. This article greatly benefited from the comments of two anonymous reviewers and from Drs. Roland A. de Szoeke and Michael A. Spall. The work of R. Matano was supported by NSF Grant OCE 0118363, NASA Grant NAG512378, and JPL Contract 1206714. Author E. D. Palma was supported by grants from CONICET (PIP-6138) and from Universidad Nacional del Sur (24/F036).

REFERENCES

Barnier, B., 1984: Energy transmission by barotropic Rossby waves across large-scale topography. *J. Phys. Oceanogr.,* **14,** 438–447.

LeBlond, P. H., and L. A. Mysak, 1978: *Waves in the Ocean.* Elsevier Oceanography Series, Vol. 20, Elsevier, 602 pp.

Matano, R. P., 1995: Numerical experiments on the effects of a meridional ridge on the transmission of energy by barotropic Rossby waves. *J. Geophys. Res.,* **100,** 18 271–18 280.

Pedlosky, J., 2000: The transmission and transformation of baroclinic Rossby waves by topography. *J. Phys. Oceanogr.,* **30,** 3077–3101.

——, and M. A. Spall, 1999: Rossby normal modes in basins with barriers. *J. Phys. Oceanogr.,* **29,** 2332–2349.

Pratt, L. J., and M. A. Spall, 2003: A porus-medium theory for barotropic flow through ridges and archipelagos. *J. Phys. Oceanogr.,* **33,** 2702–2718.

Press, W. H., B. P. Flannery, S. A. Teukolsky, and W. T. Vetterling, 1992: *Numerical Recipes.* Cambridge University Press, 818 pp.

Rhines, P. B., 1969: Slow oscillations in an ocean of varying depth, I. Abrupt topography. *J. Fluid Mech.,* **37,** 161–189.